Partial Depth Precast Concrete Deck Panels on Curved Bridges: Finite Element Analytical Model of PCPs

Colter Roskos
Paul Biju-Duval
Victoria McCammon
Todd Helwig
Oguzhan Bayrak
Patricia Clayton
Michael D. Engelhardt
Eric Williamson

Partial Depth Precast Concrete Deck Panels on Curved Bridges: Finite Element Analytical Model of PCPs

Colter Roskos
Paul Biju-Duval
Victoria McCammon
Todd Helwig
Oguzhan Bayrak
Patricia Clayton
Michael D. Engelhardt
Eric Williamson

Table of Contents

List of Figures

Introduction: Finite Element Analytical Model of PCPs

A number of full-scale tests have been carried out in the laboratory focused on the shear performance of simulated precast concrete deck panels (PCP). Shear tests were carried out to simulate the type of loading that will be applied to the deck panels as they are engaged as a bracing element. As part of the research study, two different finite element models were developed to improve the understanding of the behavior of the concrete deck panels as well as the members that are to be braced by the deck panels. The two models consist of a detailed model as well as a simple model. The purpose of the detailed model is for studying the impact of details on local stress concentrations in the panels so as to understand the potential for cracking or crushing of the concrete in isolated regions. The purpose of the simple model is to represent the stiffness and strength of the concrete deck panel for parametric studies are larger girder/bridge systems. Both of these finite element analytical models represent the most recent PCP/connection system tested in the shear frame and were developed using the commercial software program Abaqus/CAE 6.13-1. This detailed model was constructed to gain insight in the behavior of the PCP/connection system under the loads applied in the shear frame test to help refine the connection system if necessary. The simple model consists of a simple truss system that represents the PCP/connection system. This simple model will be useful for describing the PCP/connection system in the parametric finite element modeling of steel I-beam, steel tub girder, and straight and horizontally curved precast concrete box girder systems. Furthermore, the truss model will be used to represent PCP/connection systems in UT Bridge. UT Bridge is a software program that was developed as part of TxDOT research project 0-5574 and allows engineers to quickly developed analytical models of curved steel girder systems during construction. The program is currently at version 1.6; however, a major upgrade is in the works for the program that will be released at version 2.0. The simple model that is being developed as part of this project will be utilized in the program, which will provide an easy means for engineers to account for the contribution of the deck panels during the analysis of the erection or deck construction stages.

1. PCP/Connection System Overview

For the first stage of the laboratory tests, the research team fabricated reinforced concrete (R/C) deck panels to focus on the impact of various connection details on the bracing potential of the concrete deck panels. The decision to use R/C deck panels was made for practicality so that some the logistic and planning/scheduling issues that will exist with working through a commercial precaster could be avoided during the early stages. The next stage of the testing program will be carried out using commercially constructed PCPs that will be prestressed. While the panel used that have been used to date were not prestressed, an effort was made to construct the panel according to the TxDOT prestressed concrete panel fabrication details (PCP-FAB). The panel had a length of 8'-0", a width of 8'-3", and a thickness of 4 inches. The transverse reinforcement consisted of #3 grade 60 reinforcing bars spaced at 6 inches on center (this was inconsistent with the PCP-FAB details, which require prestressing strands in this direction). The longitudinal reinforcement consisted of #3 grade 60 reinforcing bars spaced at a maximum of 6 inches on center. The mix design was used for the panel had a target 28 day

strength of f'c=5000 psi, which was consistent the minimum required by the PCP-FAB. The actual test day strength (18 days) was f'c = 5.1 ksi.

As shown in Figure 1, two L4x3x3/8 angles 8'-3" long were cast into the edges of the panel (perpendicular to the span of the girders) so that the PCP could be positively attached to the loading beams. The angles were anchored to the slab using ½ inch diameter by 1'-6" long Nelson D2L deformed anchor bars. To create a tension and shear load path, the D2L anchors were lap spliced with the longitudinal reinforcement in the slab. The length of the lap splice exceeded the development length of the bars. The deformed anchors were welded to the embed angle with a Nelson stud welding gun.
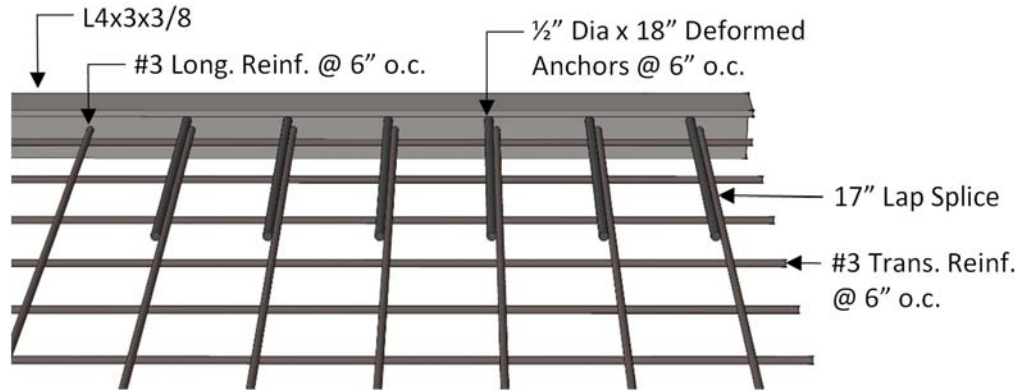
Figure 1: PCP Reinforcement Detail

After a number of iterations of tests with different details, the method of connection shown in Figure 2 was identified as the most practical and with the best performance. The connection to the girders is made with four WT 9 x 35.5 x 1'-10" long to fasten the corners of the panel to the test frame, which simulates the top flanges of two adjacent bridge girders. This 9 inch deep section was used to accommodate the panel sitting on a 4 inch tall bedding strip (the maximum bedding strip height allowed by TxDOT). The connection tees were attached to the embed angles with 18 inches of 3/16 inch fillet weld and were attached to the loading beams with 19 inches of 3/16 inch fillet weld in a C-shape.

Figure 2: PCP Connection Detail

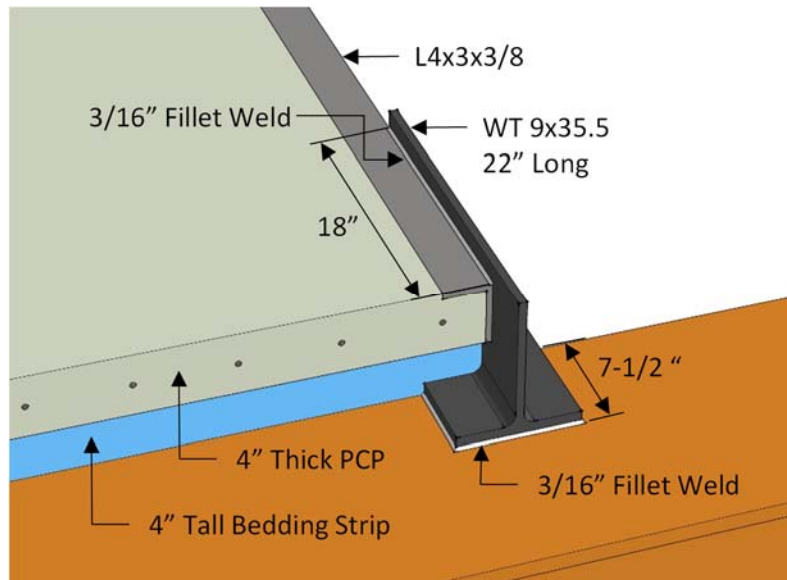## 2. Detailed Finite Element Mesh Model Parameters

2.1. Mesh and Element Type

The detailed finite element model was created using linear brick elements with reduced integration for the concrete, embed angles, tee members, and welds connecting the members as shown in Figure 3. Relatively small elements of approximately 1.5x1.5x0.5 inches were used to model the PCP resulting in eight elements through the thickness of the member. The WT9x35.5's stem was modeled with elements of approximately 0.5x0.5x0.125 inches (four elements through the thickness) while the flange of the WT was modeled with elements of approximately 0.5x0.5x0.2 inches (four elements through the thickness). The fillets of the WT members were not accounted for in the model. For the L4x3x3/8s, elements of roughly 0.5x0.5x0.125 inches were used (three elements through the thickness) in the model. The top flanges of the loading beams were modeled using rigid shell elements. Linear truss elements were used to represent the #3 reinforcing bars in the PCP and were meshed with a nodal spacing of approximately 1.5 inches.
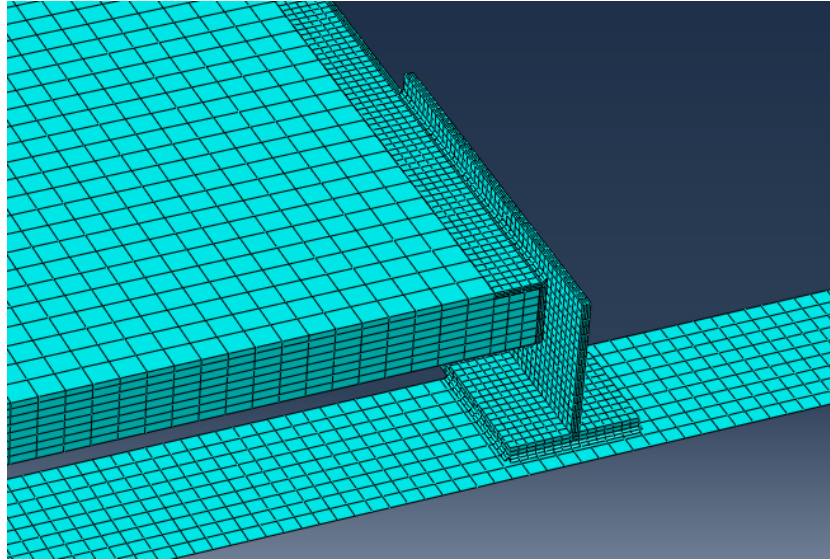
3

Figure 3: PCP Finite Element Mesh

2.2. Constraints

The geometrical complexity of the system was such that it would prove unreasonably laborious to mesh the components to join only at nodal locations. Therefore, tie constraints were used to connect the welds to the embed angles, WTs, and the loading beams. Tie constraints were also used to connect the embed angle to the concrete panel as the D2L deformed anchors were not specifically modeled in the system. Contact restraints were used to allow members of the frame contacting each other to transfer compression forces but not transfer tensile forces (the contact between the embed angle and the web of the WT was of particular importance). An embedment constraint was used to model the interaction of the reinforcing within the concrete.

2.3. Material Properties

To incorporate nonlinear material behavior, traditional metal plasticity was used to represent the steel components and the cast iron plasticity was used to represent the concrete components in the model. For simplicity, an elastic-perfectly plastic model was used to describe steel elements in the model using a Young's Modulus of 29,000 ksi, a Poisson's Ratio of 0.29, and a yield stress of 60 ksi for the reinforcement and 50 ksi for all other steel members. The cast iron plasticity model was used for the concrete since it is able to represent different strengths for the material in tension and in compression. The assumed post-yielding behavior of both compression and tension in this model is perfectly plastic. While this behavior is not realistic of the post peak softening that concrete experiences in both tension and compression, it is less costly from a numerical viewpoint. The compressive strength of the concrete was taken as $f'_c = 5.1\ ksi$ (from the test day breaks) and the concrete modulus of elasticity was calculated using the traditional equation of $E_c = 57,000\sqrt{f'c} \approx 4000\ ksi$. Values of the elastic and plastic Poisson's Ratios of 0.25 and 0.40 were used, respectively. The tensile strength of the concrete was taken as 6% of the compressive strength ($0.06f'_c \approx 0.30\ ksi$) which corresponds to roughly $f'_c = 4.25\sqrt{f'c}$. Figure 4 shows a plot of the stress vs strain for the concrete material model.
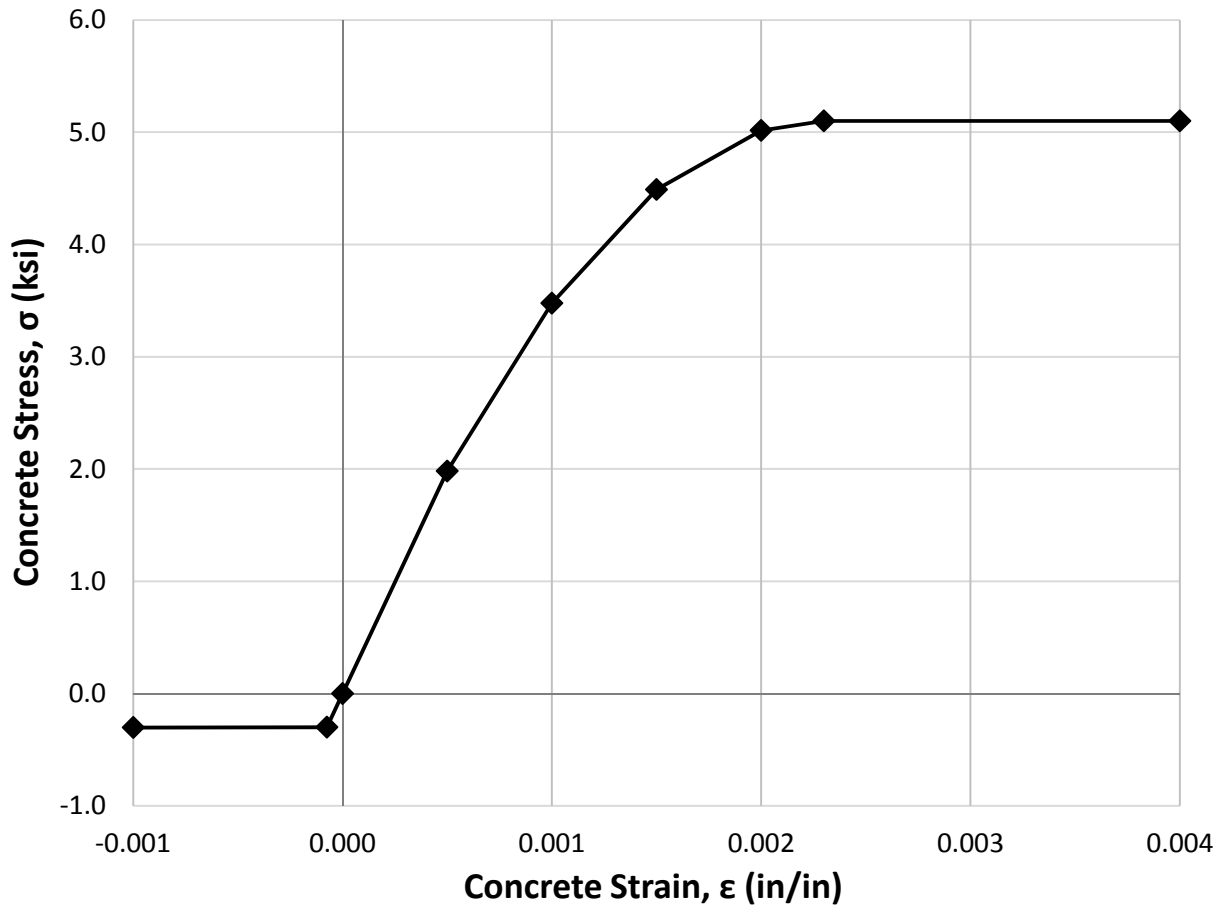
Figure 4: Concrete Stress-Strain Behavior (Cast Iron Plasticity Model)

2.4. Loading Conditions (FEA vs Laboratory)

A schematic of the shear test frame is shown in Figure 5. The two loading beams of the testing frame simulate the top flanges of either two adjacent I-girder sections or the two top flanges of a steel or concrete tub girder. As the girders in a bridge twist, the panels will restrain the relative shearing deformation of the two adjacent flanges. The laboratory test frame was designed to act as a mechanism with needle bearings at the corners to minimize friction. The shear deformation is applied using a hydraulic actuator at the end of the frame to push or pull the frame. The actuator location is identified in the figures by the arrow with the letter "P" to represent the load applied to the frame. The actuator was connected to the test frame and its reaction block via pins at both ends, allowing the connecting strap to move downward as the loading beams sway to the side. Throughout the test, the two loading beams remain parallel to one another since the connecting strap has a relatively large axial stiffness. Applying a horizontal displacement to the finite element model causes the loading beams to sway to the side but does not allow the connecting strap to move downward in the process. This loading condition attempted to elongate the rigid loading beams that caused numerical instability in the model. To resolve this issue, the finite element model was loaded by applying equal rotations (or moments) to the bottom of the rigid loading beams as shown in Figure 5.
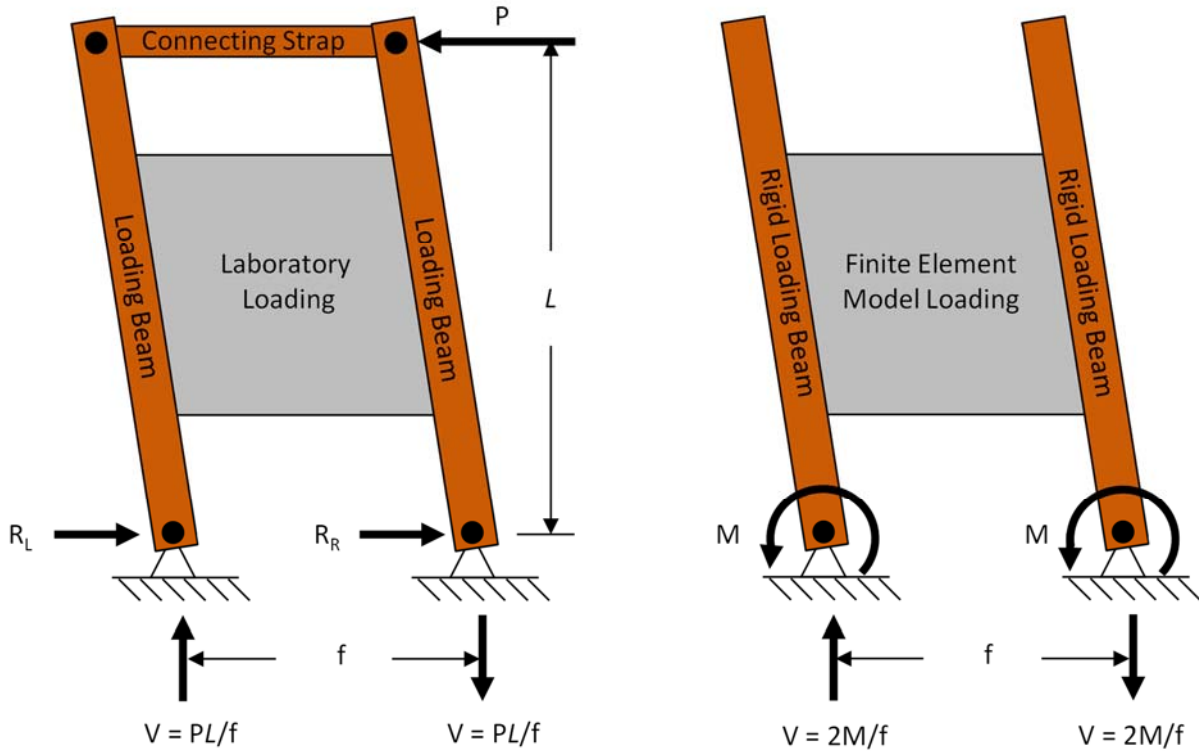
Figure 5: Laboratory vs. Finite Element Loading

2.5. Imperfections

In the test frame, the PCP can be visualized as a cross-frame with a tension brace and a compression brace as shown in Figure 6. The forces at the corners result in either a compressive or tensile load that is transferred via the connection between the PCP and the shear frame. While one component of the force at the corner is transferred to the connection parallel to the length of the WTs (CV or TV) the other component of the force is transferred to the connection perpendicular to the length of the WTs (CN or TN) as shown in Figure 7. Since the PCPs are only connected to the stem of the WTs at the top of the panel, the connection stiffness varies depending on the direction of the applied load. In tension, the stiffness can be approximated as a cantilevered beam of length L_1 loaded at the free end ($k_T = L_1^3/(3EI)$) while in compression, the stiffness can be approximated as a fixed-fixed beam of length L_2 that is allowed to deflect but not rotate at one end ($k_C = L_2^3/(12EI)$). If a gap is present between the PCP's embed angle and the stem of the WT, the stiffness of the connection in compression will equal the stiffness of the connection in tension until the gap closes ($k_{C\_gap} = k_T = L_1^3/(3EI)$).
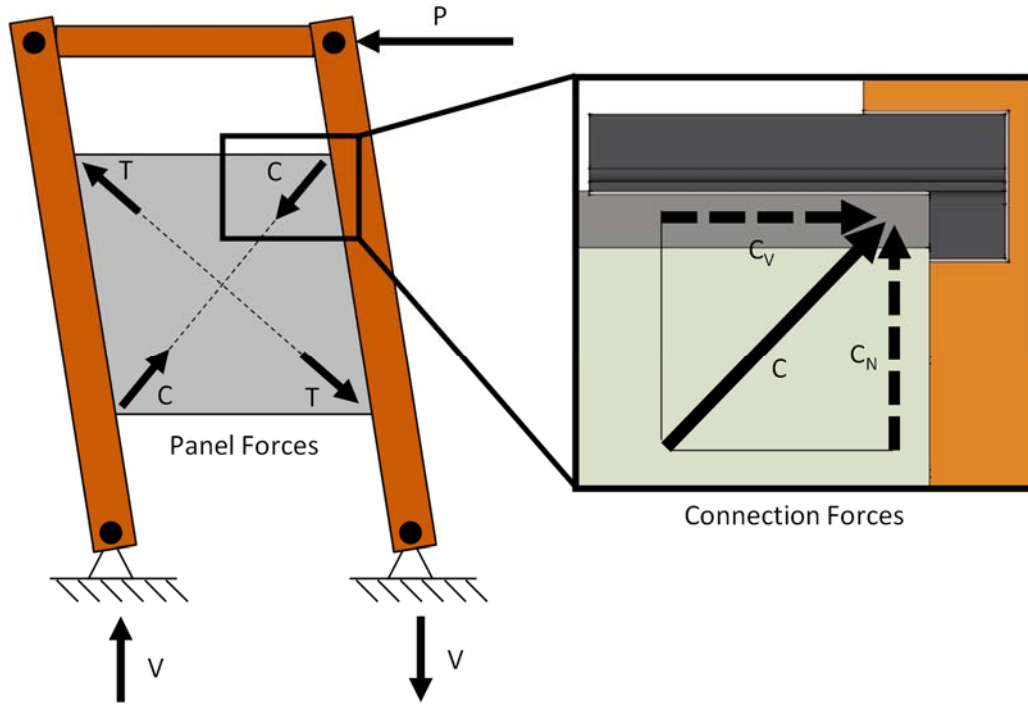
Figure 6: Shear Frame Loading

$$k_T = L_1{}^3/(3EI)$$
$$k_{C\_gap} = L_1{}^3/(3EI)$$
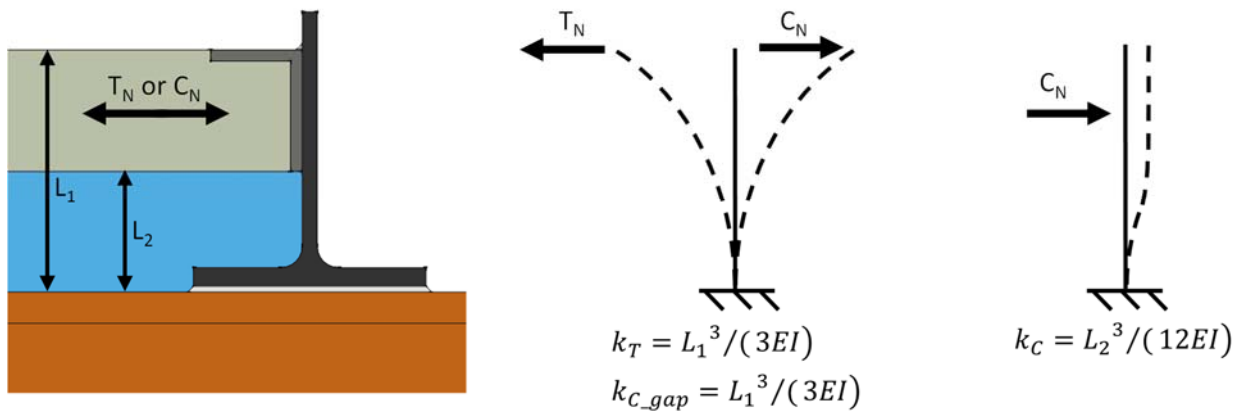
$$k_C = L_2{}^3/(12EI)$$

Figure 7: PCP Connection Stiffness Behavior

The overall stiffness of the PCP system is represented by the stiffness of springs in series where the inverse of the total system stiffness (k_{sys}) is equal to the sum of the inverse of the connection stiffness (k_{con}) and the inverse of the PCPs stiffness (k_{pcp}) as shown in Equation 1. The relationship is such that the system stiffness is always smaller than the smallest component stiffness (k_{con} or k_{pcp}). Therefore, an apparent change in the system stiffness will be seen if the connection stiffness increases (due to the closing of a gap between the embedded angle and the stem of the WT).

$$\frac{1}{k_{sys}} = \frac{1}{k_{pcp}} + \frac{1}{k_{con}}$$

Equation (1)

7

A slight gap was observed between the bottom of the vertical leg of the embed angle and the web of the WT member. Therefore, a change in the stiffness of the system was expected to be seen in the test results with the stiffness increasing after the gap closed in the system. To capture this behavior in the finite element model, a 0.05 inch gap was introduced between the vertical leg of the embed angles and the stem of the WT at one of the compression corners of the PCP. Linear potentiometers were used to measure the deflection of the stems of the WT's as the system was loaded the in the laboratory. This data was compared with deflections extracted from the finite element model as shown in the following section.

3. Finite Element Results vs. Laboratory Test Results

3.1. Effective Shear Modulus

Figure 8 shows a comparison of the shear force vs shear strain for the laboratory test results and the results from the finite element model. The dips in the laboratory test results occurred from system relaxation when the loading was paused to mark cracks in the concrete. While the FEM was unable to capture the failure mechanism of the PCP/connection system, the PCPs used in the field for bracing purposes are not expected to be loaded to this level. The slope of the stress-strain curve is defined as the effective shear modulus, G' and represents the stiffness of the system. As expected, there is an apparent change in G' in both the laboratory and FEA results as the gap between the embed angle and the stem of the WT closes. For ease of comparison, G' of the FEA and laboratory test results are represented using a tri-linear model (as shown in Figure 9) even though the effective shear modulus is not a constant after the material becomes non-linear.
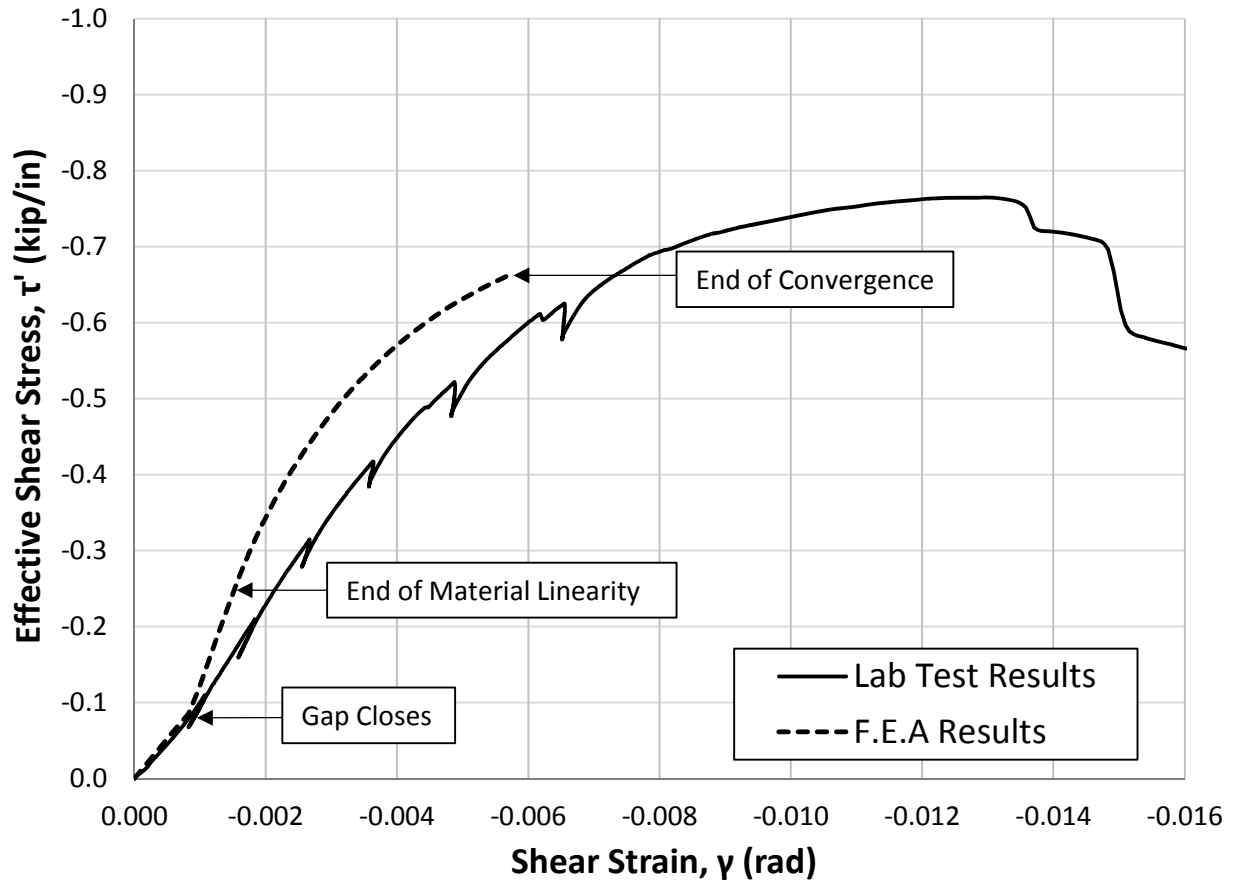
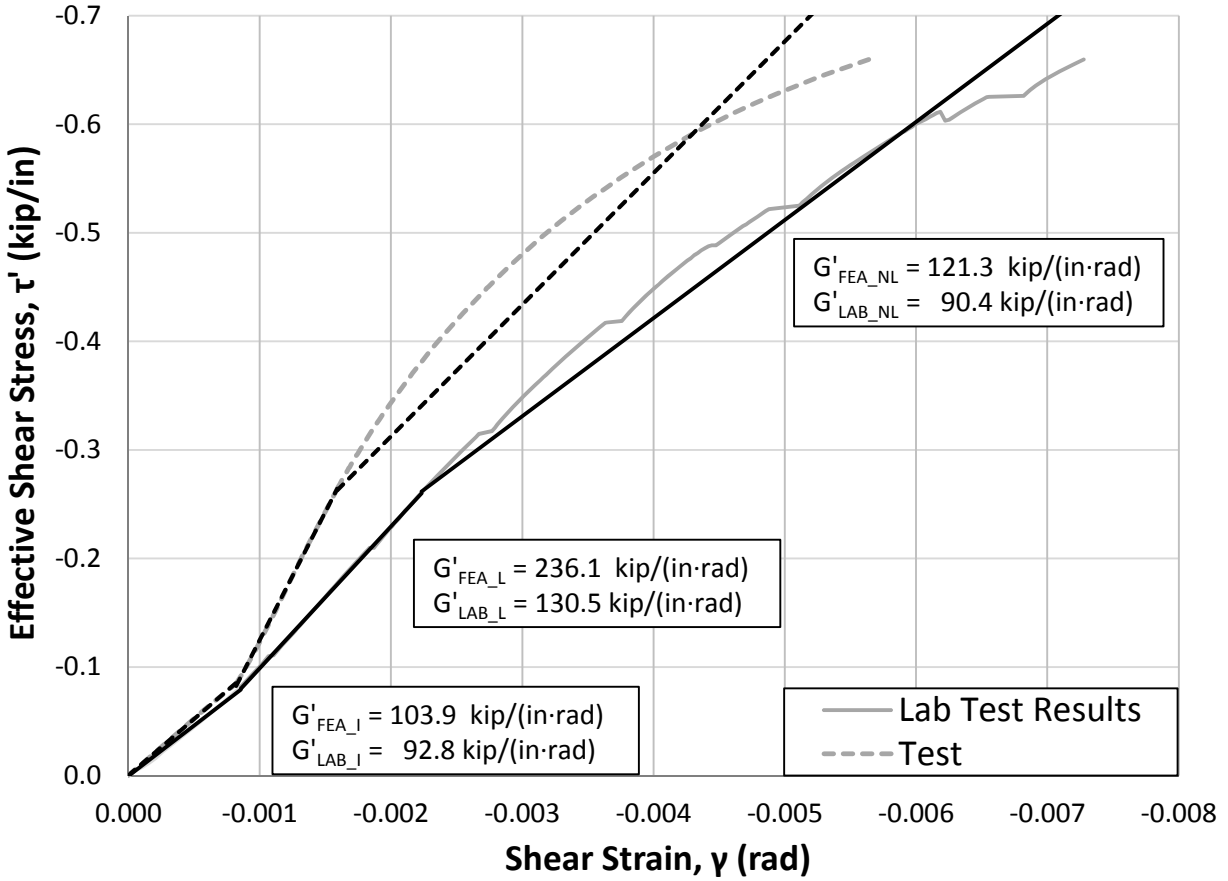*Figure 8: Comparison of FEM and Laboratory Test Data*

Figure 9: Comparison of FEM and Laboratory Test Data

In the first portion of the curve, G' for the FEM closely matched the laboratory results (G'_{FEA_1st}/ G'_{LAB_1st} = 1.12). In the second portion of the curve, largest variation in G' was seen between the FEM and laboratory results (G'_{FEA_2nd}/ G'_{LAB_2nd} = 1.81). In the third portion of the curve, G' for the FEM match the laboratory results better than in the second portion ($G'FEA\_1st$/ G'_{LAB_1st} = 1.34). In all cases, the FEM was stiffer than the laboratory results as expected since the approximate strain energy of finite element method will always underestimate the exact strain energy of the system. The large variation between G'_{FEA_2nd} and G'_{LAB_2nd} could possibly be attributed to how the connection between the embed angel and the PCP was modeled versus how it actually behaves. As aforementioned, the contact surfaces of the embed angle and PCP were connected to each other using a tie constraint in the FEM. In reality, the embed angles are connected to the PCPs at the discrete locations of the D2L anchors which will cause a reduced stiffness compared to the FEM due to elastic elongation of the D2Ls, slippage of the D2Ls in the concrete, localized crushing of the concrete at the D2Ls, etc.

3.2. Deformations in Web of WT

Linear potentiometers (L-pots) were installed at all four corners of the PCP to measure the deflections of the webs of the WTs as the system was loaded (see Figure 10). At the same locations of the L-pots, the force vs deflection curves were extracted from the FEM. The deflection at the compression corners and the tension corners are shown in Figure 11 and Figure

12, respectively. The size of the gap was adjusted at each of the corners until a similar behavior was seen between the FEM and the laboratory data. As aforementioned, a final gap of 0.05 inches was used at the NE corner of the panel.
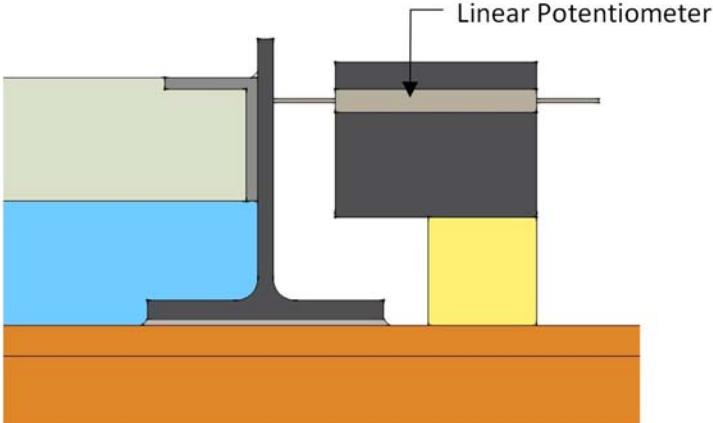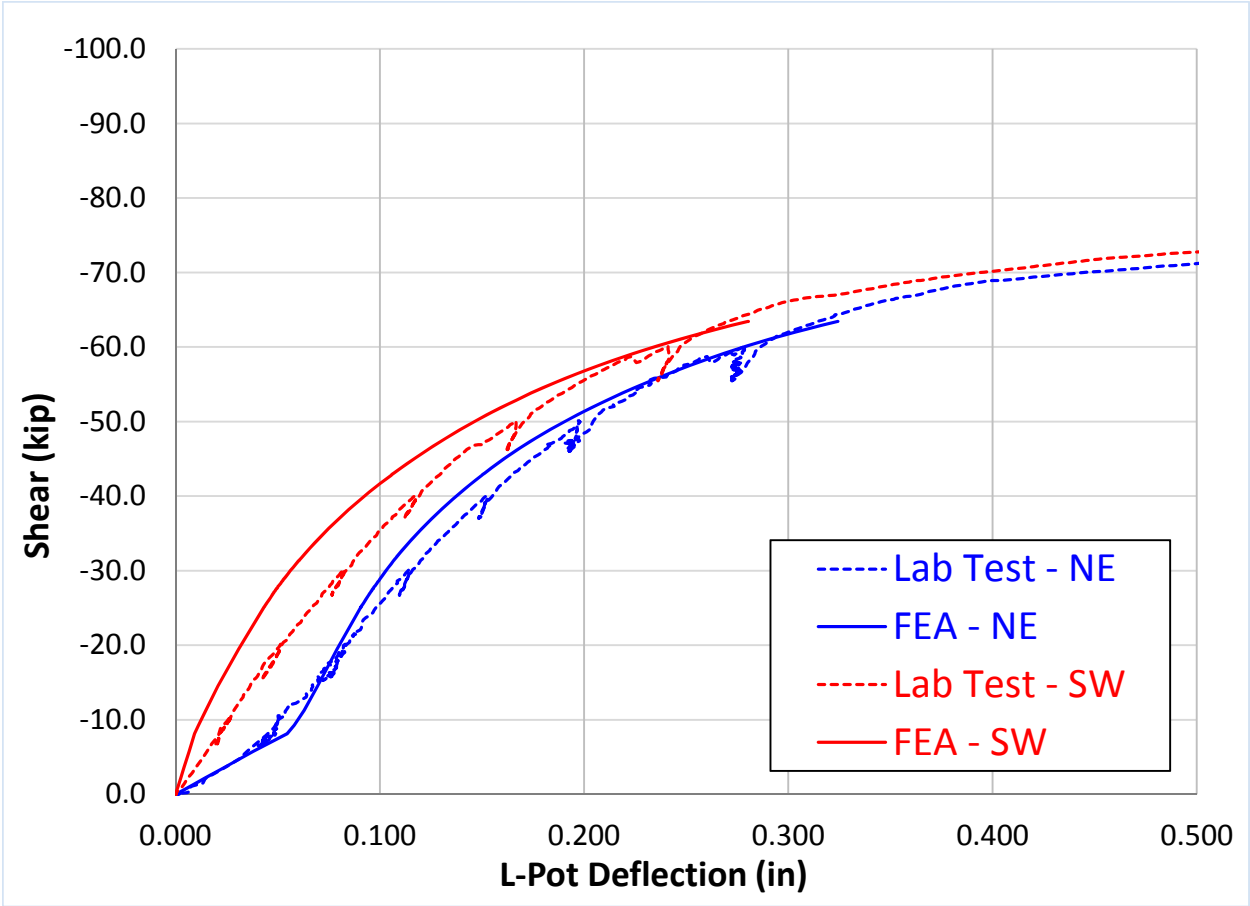

Figure 10: Connection Instrumentation

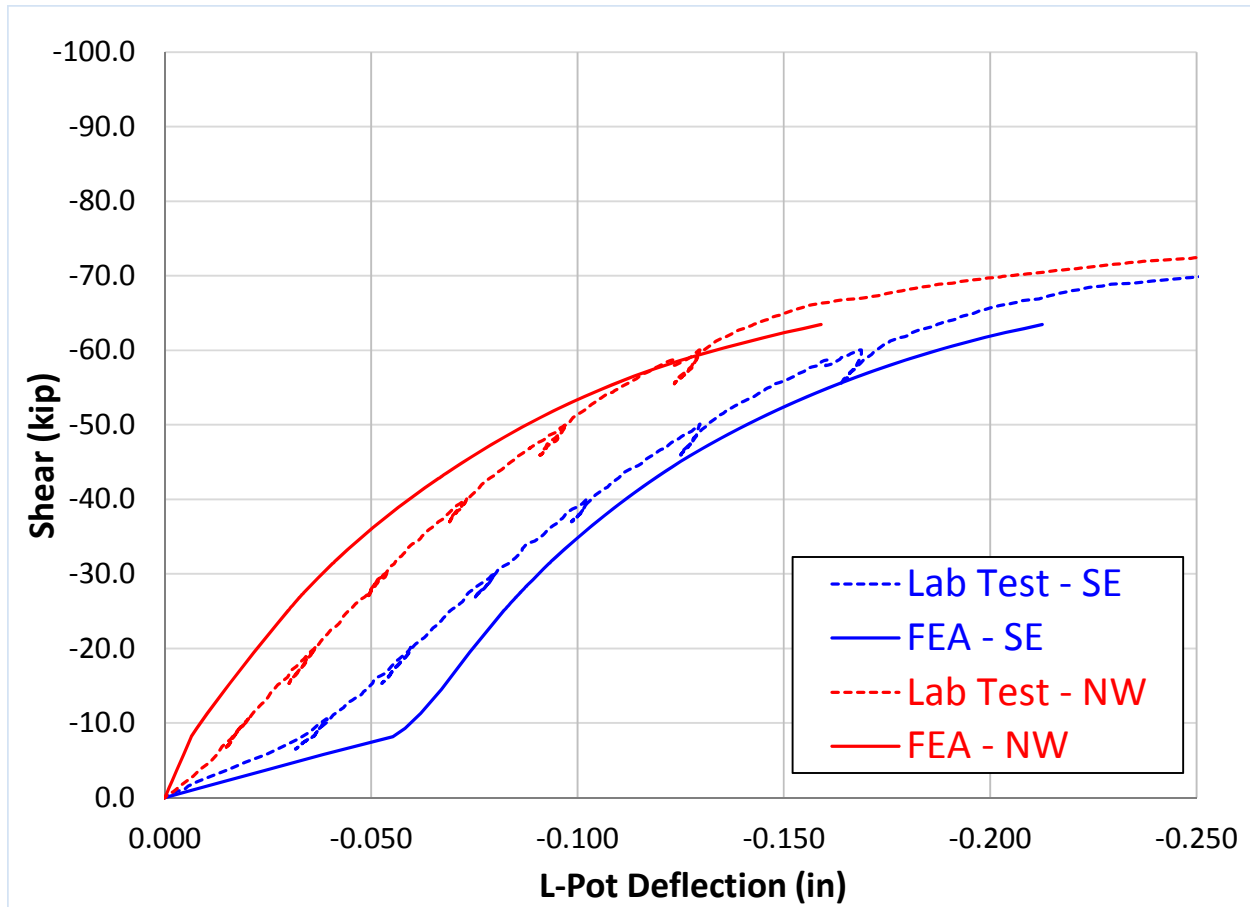*Figure 11: Force vs. Web Deflection of Compression Corners*

Figure 12: Force vs. Web Deflection of Tension Corners

4. Simple Truss Model

Helwig and Yura (2008) successfully used two-node truss elements to model shear diaphragms of light gauge metal deck forms in twin girder finite element analysis models. In a similar manner, two-node truss elements can be used as a simple model for the PCP/connection system. Using a two diagonal (X-frame) configuration, the in-plane rotational stiffness of a single panel based on work by Yura (2001) and is given as:

$$\beta_b = \frac{AEw^2f^2}{L_d^3} \qquad \text{Equation (2)}$$

where β_b = rotational stiffness of truss panel (kip-in/rad); A = diagonal area; E = elastic modulus; w = strut spacing; f = girder spacing (centerline to centerline); and L_d = diagonal length. Figure 13 shows a free body diagram of the X-frame model in a twin girder system. The shear rigidity of a panel, Q, is calculated by dividing the rotational stiffness, β_b, by the center to center spacing of the panels along the bridge. If the panels are located adjacent to one another, then Q=β_b/w. Combining the equation β_b=M/γ with G'=V/(γw) and Equation (2) above, the area of the truss elements can be derived as follows:

12

$$A = \frac{G'L_d^3}{2Ewf} \qquad\qquad \text{Equation (3)}$$

$\gamma = \Delta/w$

$\beta_b = M/\gamma$

$2M = V \cdot f$

$$\beta_b = \frac{AEw^2f^2}{L_d^{\,3}}$$
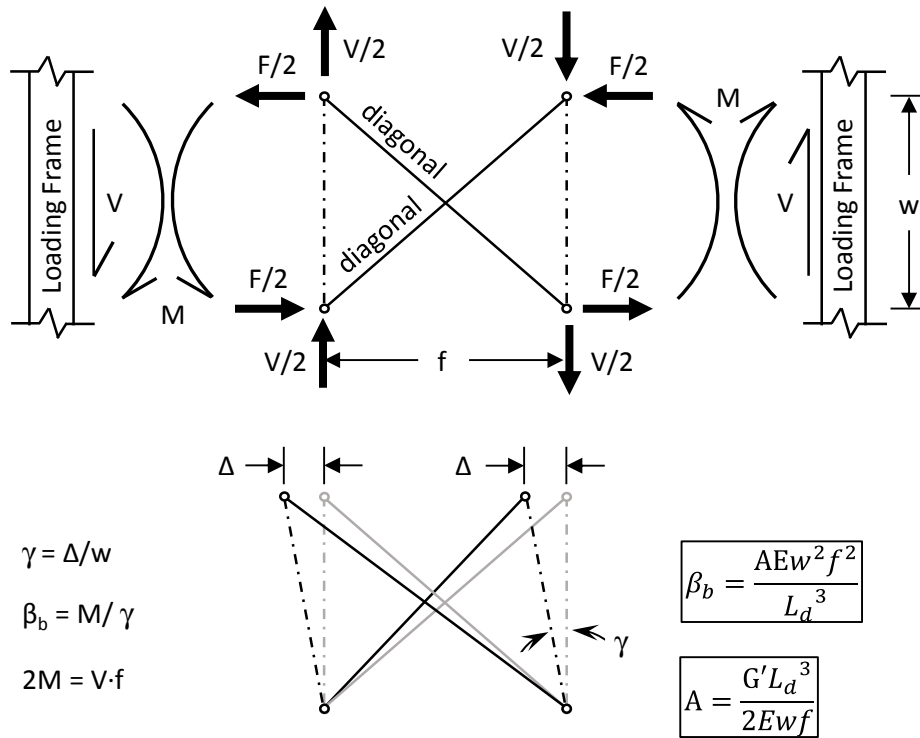
$$A = \frac{G'L_d^{\,3}}{2Ewf}$$

Figure 13: Truss Lateral Stiffness

To calculate the area of the truss elements, G' was taken as the slope of the laboratory stress-strain curve up to 60 percent of the maximum stress (G'$_{LAB\_0.6}$ = 114.9 kip/(in·rad)) as shown in Figure 14. From Equation (3) with f = 99 in, w = 96 in, L$_d$ = 137.9 in, E=29000 ksi and G' = 114.9 kip/(in·rad), the truss area was calculated to be A = 0.55 in^2. Since the PCP was not connected to the centerline of the loading beams during the laboratory test, Equation (3) slightly overestimates the area of the truss members (i.e., G' is slightly overestimated in the shear frame test). A truss area from an FEM that accounted for the X-frame connected at the same location as the PCPs in the laboratory test was found to be A$_{FEM}$ = 0.49 in^2. Figure 15 shows a screen shot of the truss finite element model.

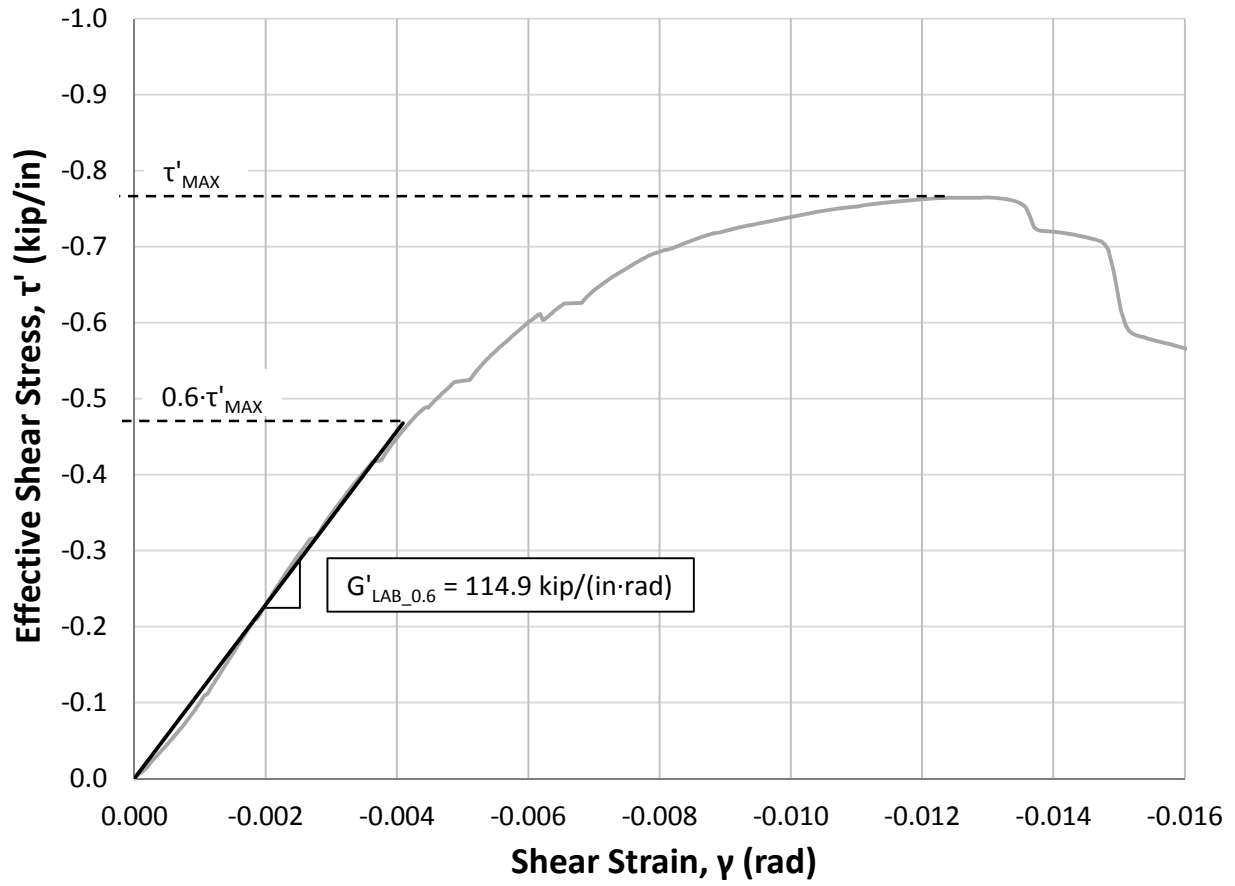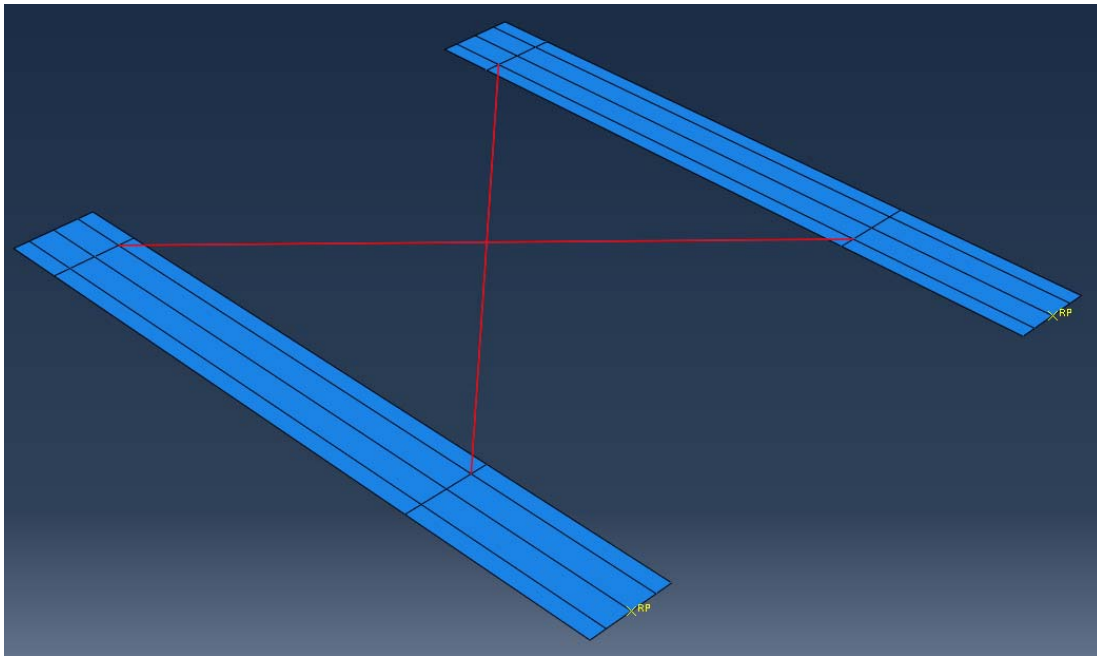*Figure 14: Effective Shear Modulus at 60 Percent of Ultimate Load*

Figure 15: Finite Element Model of X-Frame

14

5. Implementation in UT Bridge

Currently, a new version of the UT Bridge is under development. Version 2.0 uses a new quadratic isoparametric element for the webs, flanges, connecting plates and stiffeners. While UT Bridge 2.0 will have several modifications and improvements from the existing version, the research team has also included the ability for a designer to account for the PCPs' structural properties to provide additional bracing to straight or curved girders during construction. Thus, the designer can quickly investigate the benefits of using PCPs to control girder displacements during erection and to increase the buckling eigenvalue of their system during construction. In the program, a truss member can now be added between adjacent girders to represent the PCPs as described in part 4 of this report. The area of truss members can be selected by the user and for the case of the PCP modeled in this report should be taken as A=0.49 in^2.

A quick example on a twin girder system shows how implementing the equivalent trusses affects the stability of a structure. Two straight simply-supported doubly-symmetric girders of dimensions 10"x0.5" for the flanges and 40"x0.5" for the web are connected at their ends via cross-frames of cross-sectional area equal to 4.75 in^2. Without the lateral trusses representing the PCPs, the first mode is reached with an eigenvalue equal to 3.1; however, adding the PCPs with A=0.49 in^2 results in an increase in the eigenvalue to 10.6. This means it takes 10.6 times the models self-weight to cause buckling instability when a PCP is attached versus the 3.1 time the models self-weight to cause buckling instability when the PCP is unattached. See Figures 16, 17, and 18.
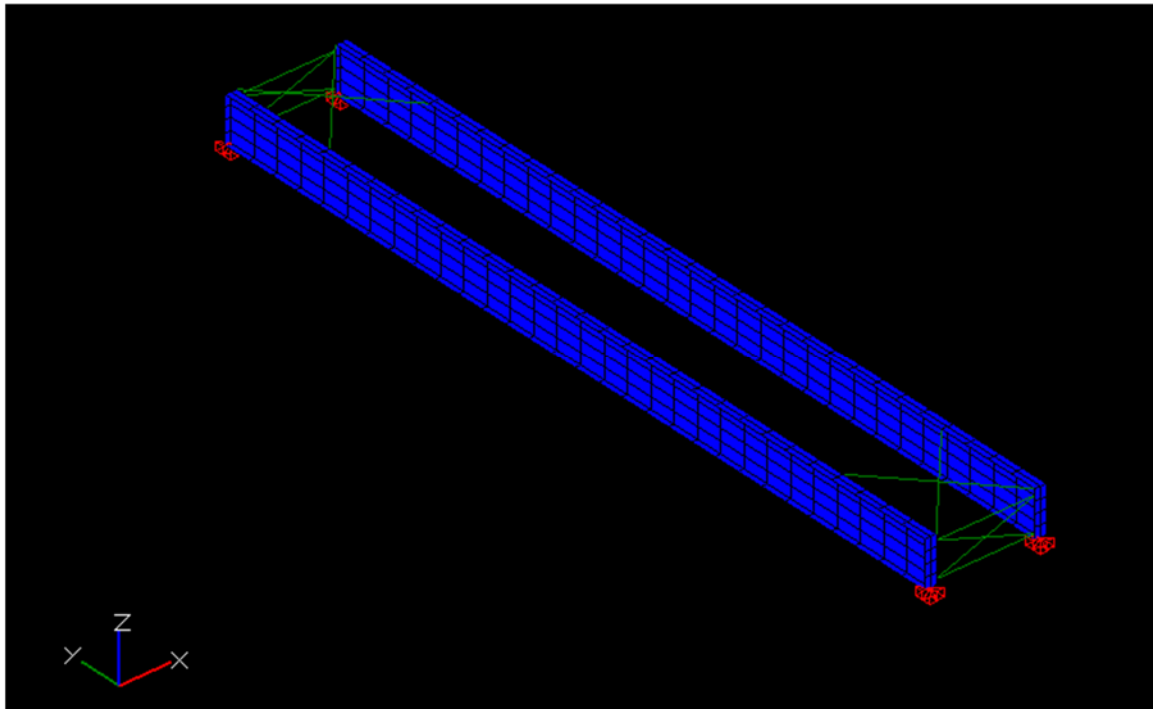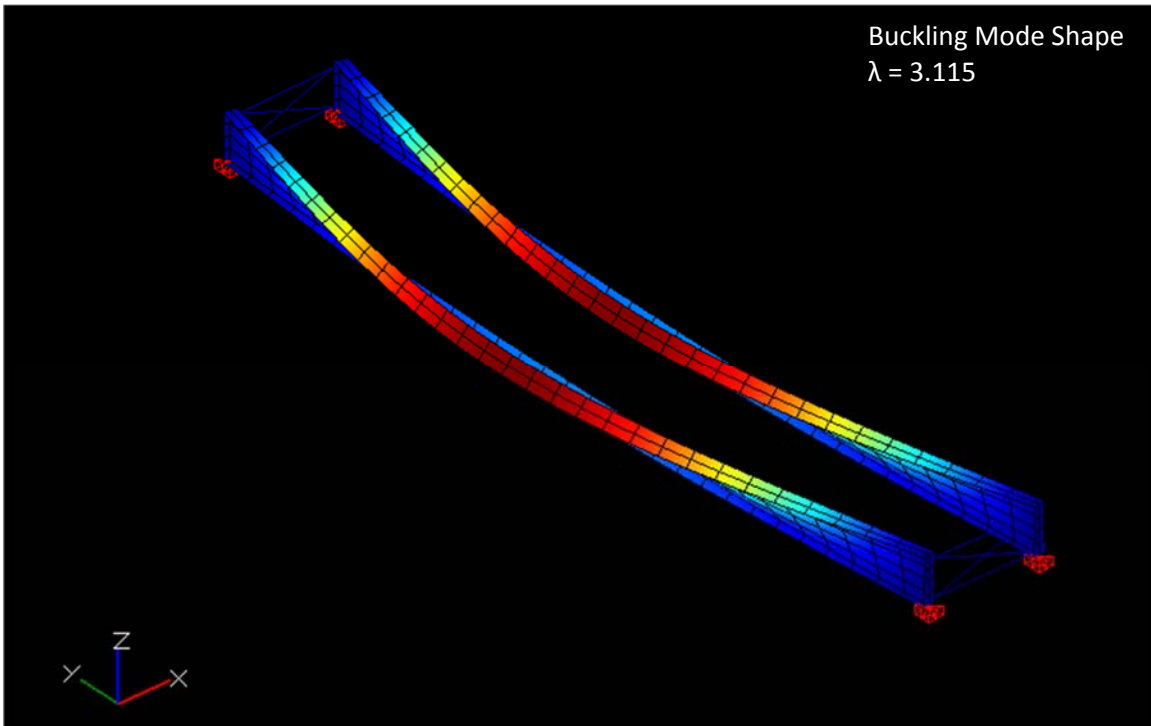

Figure 16: Modelling of the PCPs in UT Bridge

15

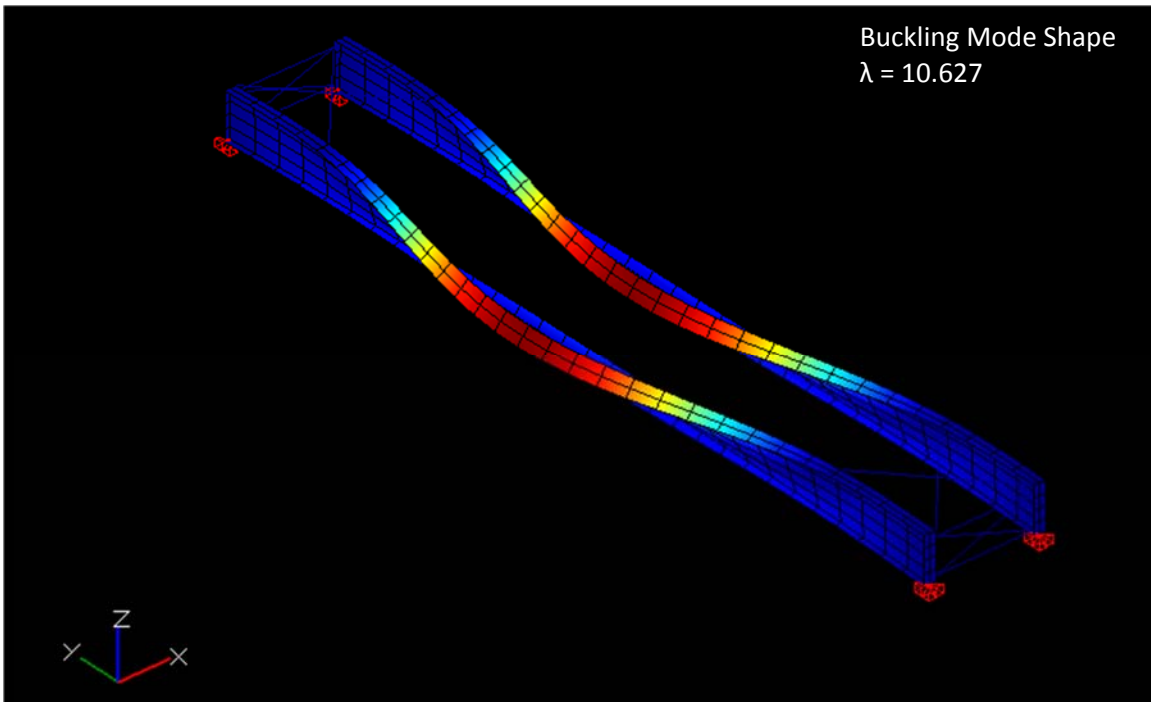*Figure 17: Buckling mode shape (without PCPs)*

Figure 18: Buckling mode shape (with PCPs)

16

6. Conclusions

A detailed 3D brick finite element model of the PCPs was produced, which provides an accurate estimate of their stiffness and strength, as measured experimentally at the large-scale laboratory tests. A simplified model consisting of 3D truss elements was also developed to provide a good representation of the stiffness and strength of the panels for use in analyses on larger systems. The truss element model is similar to previous models of permanent metal deck forms used by Helwig and Yura (2008). The simplicity of this truss model can be used in UT Bridge 2.0 or other commercial FEA programs to estimate the impact of PCPs on bridge systems, providing the designer with a better estimate of the stability and the deflections of a bridge under erection.

References

Helwig, Todd and Yura, Joseph (2008) "Shear diaphragm bracing of beams. I: Stiffness and strength behavior." *Journal of Structural Engineering*, 134(3), 348-356.

Yura, Joseph (2001) "Fundamentals of beam bracing." *Engineering Journal*, 38(1), 11-26.